NASA TM-76700

NASA TECHNICAL MEMORANDUM

NASA TM-76700

THERMAL COUPLING OF A HEAT FLUX SENSOR

Erwin Kaiser

Translation of "Die thermische Ankopplung eines Waermestromaufnehmers". Wissenschaftliche Zeitschrift, Technische Universitaet Dresden, Vol. 27, No. 3-4, 1978, pp 743-746 (A78-49174).

NATIONAL AERONAUTICS AND SPACE ADMINISTRATION
WASHINGTON D.C. 20546 MARCH 1982

STANDARD TITLE PAGE

1. Report No. NASA TM-76700	2. Government Accession No.	3. Recipient's Catalog No.
4. Title and Subtitle THERMAL COUPLING OF A HEAT FLUX SENSOR		5. Report Date MARCH 1982
		6. Performing Organization Code
7. Author(s) Erwin Kaiser		8. Performing Organization Report No.
		10. Work Unit No.
9. Performing Organization Name and Address SCITRAN Box 5456 Santa Barbara, CA 93108		11. Contract or Grant No. NASw- 3542
		13. Type of Report and Period Covered Translation
12. Sponsoring Agency Name and Address National Aeronautics and Space Administration Washington, D.C. 20546		14. Sponsoring Agency Code

15. Supplementary Notes

Translation of "Die thermische Ankopplung eines Waermestromaufnehmers".
Source: Wissenschaftliche Zeitschrift, Technische Universitaet, Dresden, Vol. 27, No. 3-4, 1978, pp. 743-746 (A78-49174).

16. Abstract

The conditions of thermal coupling are investigated in relationship to the development of sensors for local thermal flux measurements of component surfaces. The dependence of the transfer function on heat conductivity coefficient of the measured object and the influence of the contact resistance at the sensor boundaries are discussed in terms of known results and investigations.

17. Key Words (Selected by Author(s))		18. Distribution Statement Unclassified - Unlimited	
19. Security Classif. (of this report) Unclassified	20. Security Classif. (of this page) Unclassified	21. No. of Pages 11	22. Price

N82-21558 #

THERMAL COUPLING OF A HEAT FLUX SENSOR

Erwin Kaiser[1]

The conditions of thermal coupling are investigated in relationship to the development of sensors for local thermal flux measurements of component surfaces. The dependence of the transfer function on heat conductivity coefficient of the measured object and the influence of the contact resistance at the sensor boundaries are discussed in terms of known results and our own investigations. *743

1. Introduction

One possibility of experimental determination of local thermal transfer coefficients α is to measure the thermal current density $\dot{q}$ and the related temperatures according to Figure 1. Of these, in general the surface temperature is the most difficult to measure. For the experimental investigation of the perturbation of the surface temperature field by sensors, one can, for example, use electronic and photochemical infrared photographs as well as layers of cholesterine liquids. Figure 2c, d qualitatively shows the temperature drop on an applied thermmoelement. In addition, a sensor can disturb the thermal flux field within the walls if the thermal

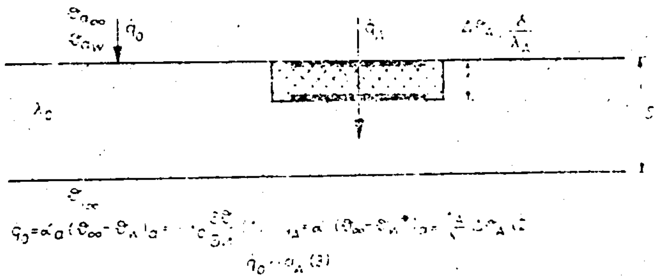

Figure 1. Auxiliary wall principle

[1]Energy conversion section, Director, Technical University, Dresden East Germany.

*Numbers in margin indicate pagination of foreign text conductivity coefficient is changed locally. For example, this occurs during temperature measurement using surface thermoelements which usually contain MgO as insulation material and they have thin metallic walls (Figure 3). During the calibration of a temperature sensor in an isothermal environment, there is no influence of the thermal conductivity coefficient difference. On the other hand, the transfer factor of a thermal flux sensor applies only for the thermal coupling condition of the calibration. Separate investigations have to be used if non-conventional materials [4] are used.

2. Thermal conduction at the measurement location

We consider the thermal flux sensors according to the auxiliary wall principle (Figure 1) of Hencky (1919) and E. Schmidt/V. Polak (1922). E. Schmidt and coworkers [8] used a one-dimensional analysis to determine the correction of the measured thermal flux, so that the ratio of the thermal flux densities in the sensor $\dot{q}_A$ and in the original wall $\dot{q}_o$ is described using the thermal resistances w. (See (4) and Figure 1.*

$$\frac{\dot{q}_A}{\dot{q}_0} = \frac{w_0}{w_0 + w_A} \quad (4) \qquad w_0 = \frac{1}{\alpha_a} + \frac{s}{\lambda_0} + \frac{1}{\alpha_i} \tag{5}$$

$$w_A = \frac{1}{\alpha_a'} + \frac{\delta}{\lambda_A} + w_K + \frac{s - \delta}{\lambda_0} + \frac{1}{\alpha_i} \tag{6}$$

(w_K = contact resistance).

This can only be assumed for large thin sensors.

Gerascenko and Fedorov [2] investigated the thermal conductivities in an infinite plane for disc-shaped sensors using the plane electroanalogy. The course of the edge of the thermal flux tube $\dot{Q}$ (also shown in Figure 3) which passes through the disc cross-section and therefore the change in the thermal flux density $\dot{q}$

*Translator's note: apparently one column of text containing equations (1) to (4) is missing from the German.

depends on the ratio of the thermal conductivity coefficients λ_A/λ_0. Just like in (4), the ratio $\dot{q}_A/\dot{q}_0$ is used for the evaluation, which in this rotationally symmetric case is formed using the square of the thermal flux width D (7).

$$k = \frac{\dot{q}_A}{\dot{q}_0} = \frac{\dot{Q}/0.25\pi D_A^2}{\dot{Q}/0.25\pi D_0^2} = \frac{D_0^2}{D_A^2} . \tag{7}$$

Tuck [10] reports about the exact calculation of the ratio $\dot{q}_A/\dot{q}_0$ for axisymmetric sensors in an infinite surrounding. For the shape family of disc shaped sensors, the following approximate equation (8) has been given:

$$\frac{\dot{q}_A}{\dot{q}_0} = 1 + \chi\varepsilon\left(1 - \frac{\lambda_0}{\lambda_A}\right). \tag{8}$$

For thin sensors the shape parameter χ is close to π/2. The factor ε is the ratio of the greatest thickness to the largest diameter (δ/D).

(8) allows one to calculate the dependence $\dot{q}_A/\dot{q}_0 = F(\lambda_A/\lambda_0)$ calculated by Gerascenko/Federov [2] using the electro analogy (Figure 4). From all of these results one can see that the proportionality factor of $\dot{q}_A \sim \dot{q}_0$ (3) only takes on the value of 1 for the case $\lambda_A = \lambda_0$ and the thermal flux distortion in the range $\lambda_A/\lambda_0 < 1$ depends substantially on the thermal conductivity coefficient ratio. 7

3. Application

When using surface conductor material as a thermal flux sensor [4], the two temperature sensors, thermoelements or resistance thermometers are isolated by MgO powder and this is surrounded with a steel pipe. For this geometry, the calculation of Tuck [10] do not apply and, therefore, for the modeling the plane electro analogy with potential paper is used. The inhomogenization was carried out up to the thermal conductivity ratio 1:5 by Lochraster [3,7] and the relaxation method was used. According to the results (Figures 3,4)

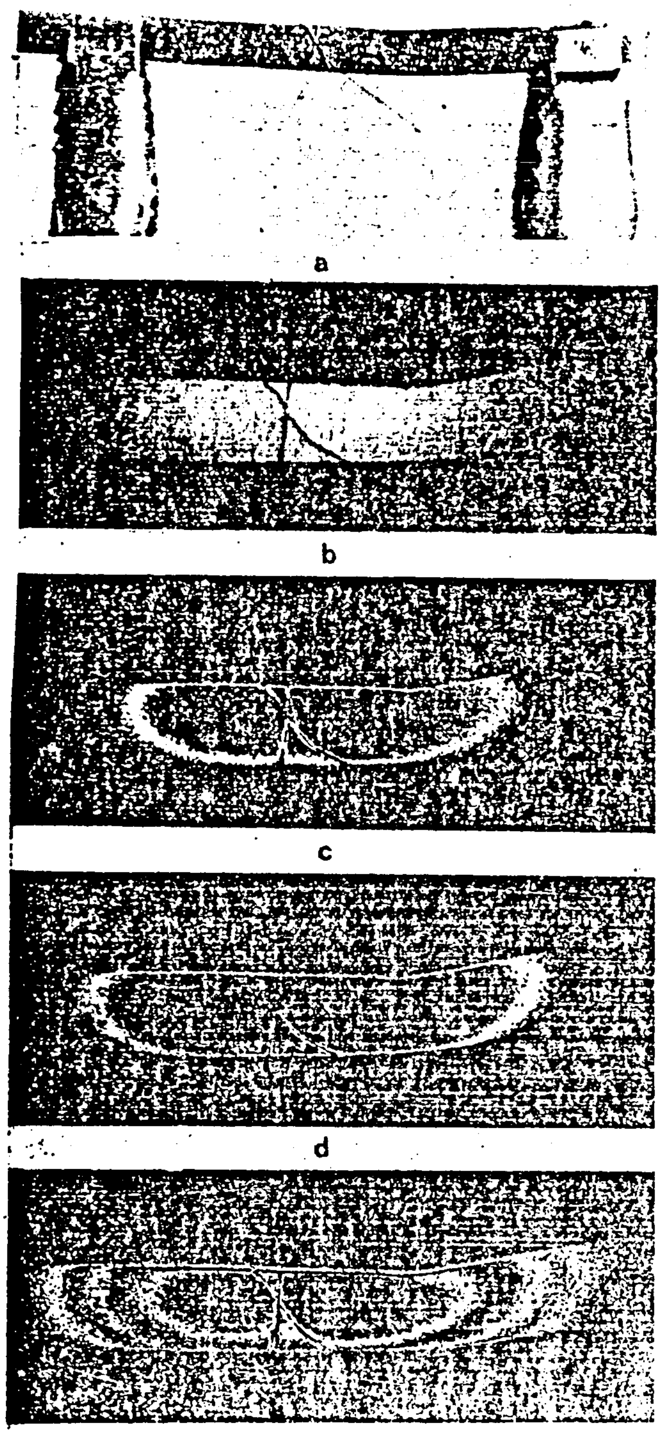

Figure 2. Infrared photography

a) photograph of a cold CrNi heating band (3x0.1 mm) with a NiCr-Ni thermoelement (0.1 mm diameter) on normal film

b) photograph at 430°C without additional light on a NI 750 small image film (f stop 2, exposure 90 seconds, 40 mm telescopic extension for 50 mm focal length)

c,d) equidensity lines of first order produced with a Sabattier effect [1] and considered as isotherm

e) combination of 3 individual equidensity curves

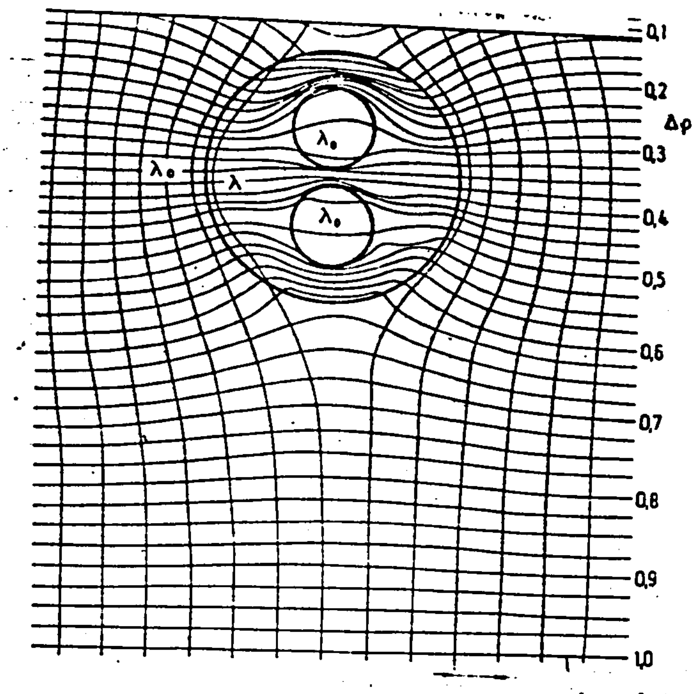

Figure 3. Isotherms (potential φ) and thermo streamlines around a cover conductor (1 mm diameter), determined with inhomogenized potential paper (model scale 200:1:4.4 mm, hole iron and 5 mm mesh distance)

the thermal flux distortion evaluated with the ratio $\dot q_A/\dot q_0$ by sensors made of cylindrical covering conductor material is about as large as the one for thin disc shaped sensors.

With this relationship, we can discuss the following optimization problem. The temperature difference $\Delta\vartheta_A$ of the sensor is to be large, but on the other hand, the ratio $\dot q_A/\dot q_0$ should not be too much different from one. Using the temperature difference $\Delta\vartheta_A$ in the sensor (2) and the temperature difference $\Delta\vartheta_0$ over a layer having the same thickness in the wall, we form the quotient (9).

$$\frac{\Delta\vartheta_A}{\Delta\vartheta_0} \quad \frac{\lambda_0 \dot q_A}{\lambda_A \dot q_0} \qquad (9)$$

which can be obtained from the dependence $\dot q_A/\dot q_0 = F(\lambda_A/\lambda_0)$ (Figures 4 and 8). The representation of $\Delta\vartheta_A/\Delta\vartheta_0 = f(\lambda_A/\lambda_0)$

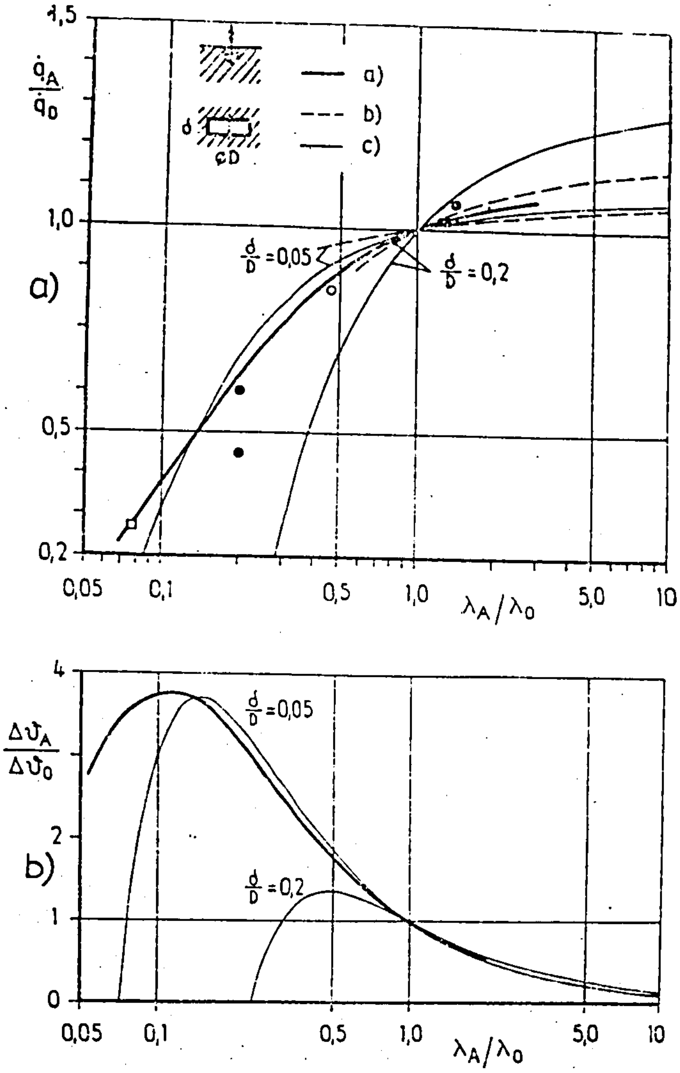

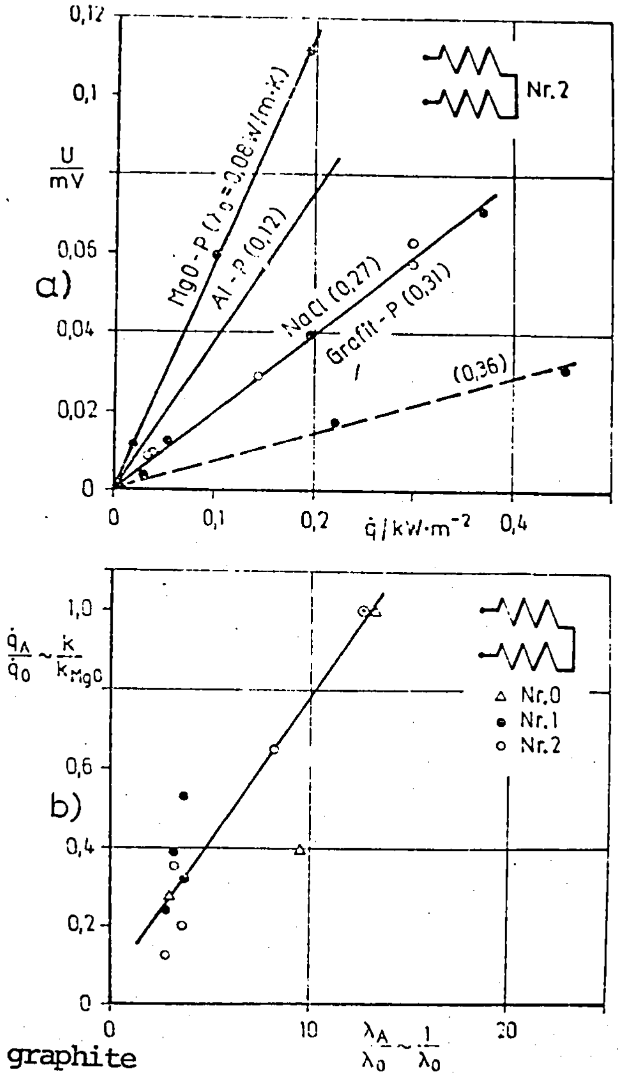

Figure 4. (Left). a) Conductivity [illegible] for cover conductors using the electrical analogy and relaxation calculation (curve a) for disc shape sensors using the electroanalogy [2]. (curve b) and two-dimensional calculation [10] (curve c).
b) ratio of temperature gradients in the auxiliary wall and surrounding [illegible] determined using curves a and c of Figure 4a.

Figure 5. (Right). a) dependence of output signal of a sensor type which transmits material [4] on thermo conductivity coefficient of the surroundings, measured with a thermo conduction test stand using the plate method. b) transmission factor K of sensor design (no. 0,1,2).

in Figure 4 shows that the increase of the transmission factor which is possible in the range $\lambda_0 - \lambda_1$ depends substantially on the ratio λ_1/λ_0.

The average thermal conductivity coefficient of the cover conductor* of λ_A 6.86 W/mK does not correspond to the effect of auxiliary wall in a vicinity, whose thermal conductivity coefficient is about as large as that of the metallic components. For an extrapolation of the tranmission factor K to higher temperatures, it is therefore assumed that the largest fraction can be described by the temperature dependence of the MgO thermal conductivity coefficient. The entire temperature dependence can be summarized as follows using (2) and Figure 4 and (7), (8) for disks:

$$\frac{K(\vartheta)}{K(\vartheta_0)} = \frac{\lambda_1(\vartheta_0)}{\lambda_1(\vartheta)} \cdot \frac{\delta(\vartheta)\, F\left[\frac{\lambda_A}{\lambda_0}(\vartheta)\right]}{\delta(\vartheta_0)\, F\left[\frac{\lambda_A}{\lambda_0}(\vartheta_0)\right]} \qquad (10)$$

For the MgO thermal conductivity coefficient, we determine the following from the mentioned values (11):

$$\lambda(100\,^\circ C)/\lambda(\vartheta) = 1{,}93 - 0{,}202 \ln \vartheta \qquad (11)$$

The differences between the values of Gerascenko/Fedorov and Tuck for homogeneous disks as well as the differences of the λ_A/λ_0 values for inhomogeneous models of a cover conductor led to the estimation that the dependence $\lambda_A/\lambda_0 = F(\lambda_A/\lambda_0)$ in Figure 4 reflect the principle relationship, but it is still too rough for corrections.

4. Experimental results

* Cross section rastered and individual resistances are added. With the determinied porosity of $P_0 = 0{,}30$ MgO powder thermal conductivity we extrapolated to $\lambda(100\,^\circ C) = 0{,}98$ W/mK. Field covering $\lambda = 13$ W/m·K. Wires $\lambda \approx 32$ W/m·K.

The following values show the influence of the surrounding thermal conductivity coefficient λ_o and the problem of the external contact resistance.

sensor	$\frac{\lambda_o}{W/m \cdot K}$	contact	$\frac{U/q_o}{mV/kW \cdot m^{-2}}$
cover thermal element (1 mm diameter)	Acryl 0.18	oil	0.0062
	steel 52	hard solder	0.0042
	steel 52	Ag powder in oil	0.0008

For perfectly soldered covered thermoelements, the contact resistance is of no importance. The materials of modern thermal installation allow welded or soldered contacts to a lesser and lesser extent. The contact resistance at the boundary MgO-powder and the steel cover is small. Malang [6] gives the contact coefficient as $25 \cdot 10^{4}\ W/m^2 \cdot K$. At the cover thermoelement steeling points after welding, these contact coefficients and the MgO thermal conductivity coefficients for the cover conductors are probably never achieved again*.

When investigating sensors in a thermo conductivity test stand, the thermo conductivity coefficient λ_o was varied using powder materials. For a sensor [4] which for the most part let materials pass through, we found a reproducable overall picture (Figure 5).

5. Conclusions

A thermo current sensor can only record the thermal flux which penetrates through it. Its applications evaluated according to the measurement range and the measurement objects, depend on the temperature difference measurement, the geometric shape, thermal conductivity coefficient and the contact with the measurement object.

---

*Thomson/Fenton [9] reported about a coaxial cover thermoelement where the thermo location is produced before covering.

The calibration should be performed on the measurement object if possible or should be included in the solution of the measurement task when the thermal coupling cannot be reproduced with certainty.

REFERENCES

[1] Botschen, R.: Equidensity curves of first order. Wiss and Fortschritt, Berlin 24 (1974), p 384

[2] Fedorov, V. G. Thermal measurement in the food industry. Moscow. Piscevaja promyslennost 1974

[3] Hackeschmidt, M. Fluid mechanics. Similarity and analogy models, Leipzig, VEB Deutscher Verlag fuer Grundstoffindustrie 1972.

[4] Kaiser, E. Local thermal flux measurement using cover conductor strip technology and strain gauge technology. messen-stenern-regeln, Berlin 21 (1978) 1, p 25

[5] Landolf-Boernstein. Numerical values and functions. Berlin, Heidelberg, New York; Springer Verlag 1972, vol. 4 part 4 p 458.

[6] Malang, S. Cover thermoelements using boron nitride insulation, atomwirtschaft, Duesseldorf 17 (1972) 4, p 155

[7] Quellmalz, W. Determination of temperature and thermal flux distribution in a thermal flux measurement device using electrical analogy. TU Dresden, sekt. 12, LG messtechnik, Dpl. Arb 1976.

[8] Schmidt, E., Werneburg, J. Thermal flux measurement for high temperatures. Zeitschr. d. VDI, Berlin 78 (1934 11, p 343.

[9] Thomson, A., Fenton, A. W. High integrity, small diameter mineral insulated thermocouples, in: Temp. Measurement, Teddington 1975.

[10] Tuck, E. O. A Theory of the Design of thin heat flux meters. Journal Engineering Math. 6 (1972) p 355-368.

End of Document